Published in Nuclear Fusion 61 (2021) 056003 (10pp); https://doi.org/10.1088/1741-4326/abecca

Dependence of blistering and deuterium retention on damage depth in damaged tungsten exposed to deuterium plasma

Shiwei Wang[1,2], Wangguo Guo[3], Long Cheng[1,2], Thomas Schwarz-Selinger[4], Mi Liu[1,2], Xiuli Zhu[5], Yue Yuan[1,2], Engang Fu[6] and Guang-Hong Lu[1,2]

[1]School of Physics, Beihang University, Beijing 100191, China

[2]Beijing Key Laboratory of Advanced Nuclear Materials and Physics, Beihang University, Beijing 100191, China

[3]Institute of High Energy Physics, Chinese Academy of Sciences, Beijing, 100049, China

[4]Max-Planck-Institut für Plasmaphysik, Boltzmannstr. 2, D-85748 Garching, Germany

[5]School of Nuclear Science and Engineering, North China Electric Power University, Beijing 102206, China

[6]State Key Laboratory of Nuclear Physics and Technology, School of Physics, Peking University, Beijing 100871, China

E-mail: LCheng@buaa.edu.cn

Abstract

The effect of different damage depth on blistering and deuterium (D) retention has been investigated in heavy-ion-damaged tungsten (W) with exposure to D plasma (40 eV, 1×10^{22} ions $m^{-2}s^{-1}$) at 550 K. Different damage depths are realized via copper (Cu) ion irradiation with energies of 1, 3, and 6 MeV on W samples with the same calculated peak damage level of 0.5 dpa. The plasma-induced blister density reduces with increasing damage depth, which is explained based on the recently proposed dislocation nucleation mechanism of blistering. Comparison of D retention measured by nuclear reaction analysis (NRA) and thermal desorption spectroscopy (TDS) reveals that retention at depths larger than 7.4 μm - which is far beyond the ion damage depth - increases with damage depth. Such a phenomenon indicates a gradual increase of diffusion flux inside the damaged sample with the increasing damage depth. It is suggested that it originates from the observed difference in blister density. Besides the widely acknowledged enhanced D retention due to ion damage, this work shows a strong impact of the damage depth on blistering such as the blister density, and by which the D diffusion flux inside W and total D retention are further affected.

Keywords: tungsten, heavy-ion irradiation, deuterium plasma, damage depth, deuterium retention, blister, linear plasma device

1. Introduction

Tungsten (W) is recognized as one of the most promising plasma-facing materials (PFMs) in ITER, demonstration fusion reactor (DEMO), or even future fusion reactor due to its unique characteristics such as low fuel retention, low sputtering yield, high thermal conductivity, and high melting point. As a PFM, W will be irradiated with a high flux of hydrogen isotopes (HIs), helium (He), neutrons, and high-heat flux, which results in a significant degradation in the overall material performance and ultimately shortens its service lifetime [1–4]. HIs behavior in W has always been the research focus since H-induced blistering and HIs retention not only degrade material properties but also affect fuel self-sufficiency of tritium (T) [3,4]. Moreover, fuel retention is expected to be aggravated in damaged W due to the abundant defects generated by neutron irradiation [5,6]. Hence, the understanding of HIs transportation and retention in damaged W is an indispensable step to evaluate the performance of PFMs under extreme conditions.

Blistering is a typical surface morphology modification in W after HIs plasma exposure, which is considered to take place because of the oversaturation of solute HIs atoms in the near-surface region, leading to crack formation in the grain interior or boundary. Up to now, several blistering mechanisms in metals are proposed such as plastic deformation, loop punching, vacancy nucleation [7,8], and dislocation nucleation [9], which are all related to crystallographic defects. Our previous study shows a reduction of the blister density in copper (Cu) damaged W samples after exposure to low-energy (40 eV) deuterium (D) plasma with a high-flux of ~1×10^{22} ions $m^{-2}s$ at both low fluence of 1×10^{26} m^{-2} and high fluence of 2.2×10^{27} m^{-2} at ~500 K [10]. A similar phenomenon is also observed in argon (Ar)- and self-damaged W samples after D plasma exposure [11–13]. As experiments were usually carried out using ion beams with a single energy, it is unclear whether this phenomenon will maintain the status quo or be altered as the damage depth increases, which is important for evaluating the effect of neutron irradiation on D-induced blistering.

The increase of the defect density in the damaged W can enhance total HIs retention which has been widely acknowledged [10,11,14–20]. In addition to retention, HIs transport in damaged W is also influenced by heavy-ion irradiation-induced defects. It has been reported

that increasing the density of defects will reduce the HIs effective diffusivity in the bulk because of the increased probability of trapping, and such an effect is likely to vanish after the displacement-damaged layer is filled [19]. Following this idea, compared with the undamaged case, less D atoms will diffuse into a larger depth in the damaged case at a given exposure condition since D diffusion to a larger depth will be suppressed until the damaged zone is filled. However, the observation of relatively large-sized blisters in the damaged case suggests indirectly that this is not the case. As demonstrated in [20], the nucleation depth of blisters in undamaged W is suggested to be at a depth ranging from about 1.0 to 2.1 μm. In contrast, large-sized blisters with a mean nucleation depth of about 10.7 μm are observed in damaged W under the same exposure condition of D plasma. Furthermore, it is inferred that the solute D concentration at a depth of 10.7 μm is high enough to trigger blister nucleation in damaged W, which means the diffusion flux near that depth is higher in damaged W than in undamaged W during plasma exposure at a flux of 10^{22} $m^{-2}s^{-1}$. The unclear formation mechanism of large-sized blisters at large depth originates from the lack of understanding in the HIs transport mechanism in damaged W. Much attention is usually paid to the inhibitory effect of displacement-damaged defects on HIs transport, while the combined effect of the displacement damage and the change in the blister density caused by displacement damage on HIs transport is usually not well investigated. Previous studies show that near-surface blisters could reduce the D diffusion flux into larger depth by enhancing D re-emission from the near surface [21,22]. From this point of view, a reduction of the blister density may lead to the change of HIs transportation through the material. Therefore, the effect of blister density changes due to displacement-damage-produced defects on HIs transport and retention needs further investigation W.

In this work, the effect of the damage depth on D-induced blistering and retention in damaged W is investigated. At present, heavy-ion irradiation with incident energies ranging from keV to MeV is widely utilized to investigate displacement damage caused by neutron irradiation due to the lack of the fusion neutron source and difficulty in handling radioactive samples [10–20,23]. Here Cu ion irradiation with different incident energies was used to obtain samples with various damage depths. After Cu irradiation, the samples were exposed to high flux D plasma in the linear plasma device STEP. Optical microscope (OM) and scanning

electron microscope (SEM), nuclear reaction analysis (NRA), and thermal desorption spectroscopy (TDS) were employed to analyze the surface modification, derive the D depth distribution, and measure the total D retention, respectively.

2. Experiment

Polycrystalline rolled W samples (purity >99.95 wt.%) purchased from ATTL Advanced Materials Co., Ltd. China with a dimension of 10×10×1 mm^3 were used in this work. The grain size is ~5 μm on the exposed surface along the rolling direction and ~2 μm along the perpendicular direction. To obtain a mirror-like surface, all the samples were mechanically polished using emery paper then electropolished using aqueous 1 wt.% NaOH solution. Annealing at 1273 K for 1 hour was performed in a high vacuum background (< 10^{-3} Pa) for outgassing and stress-relieving.

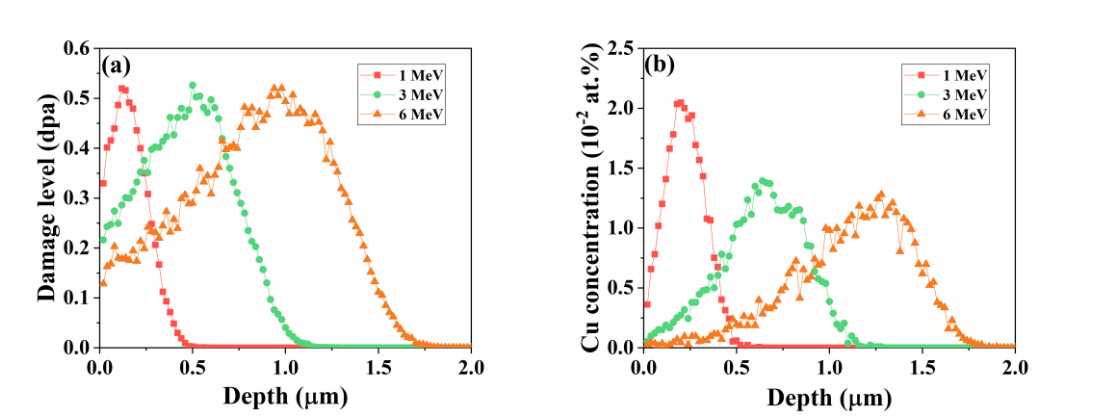

Figure 1. Damage depth profile (a) and Cu concentration (b) after Cu irradiation with three incident energies of 1, 3, and 6 MeV as calculated using the SRIM code. The applied Cu ion fluences are listed in Table 1.

Cu ions with three incident energies of 1, 3 and 6 MeV were utilized here to obtain W samples with different damage depths. Implantation was performed at room temperature (RT) at the NEC5SDH-2 2×1.7 MV tandem accelerator in the State Key Laboratory of Nuclear Physics and Technology, Peking University. Samples were glued on a Cu holder by a conductive adhesive tape, and then the holder was installed in the beam line. The Cu ion beam was scanned over the sample surface to achieve a laterally homogenous implantation. The implanted area is defined by a Cu mask with an opening of 12 mm × 12 mm. This procedure guarantees that the

entire surface of the sample is fully covered by the Cu ion beam. The option of Ion Distribution and Quick Calculation of Damage in the SRIM code was chosen to calculate displacement events as recommended by Stoller et al. [24–26]. It is important to emphasize that the option of Detailed Calculation with full Damage Cascades was chosen in our previous study [10], which leads to twice the dpa (dpa is displacements per atom) at the same Cu fluence compared with the currently applied option (1 dpa previously vs. 0.5 dpa at present) [24]. Hence, the actual displacement damage in our previous study was the same as in the present study. The displacement threshold energy (E_d) of W was set to 90 eV [15,27]. The damage level was calculated by using the equation: dpa = $N_d \Phi/N_w$, in which N_d, Φ and N_w are the number of displacements given by the SRIM code, the ion dose and the atomic density of W (6.338×10^{28} atoms/m^3), respectively. As shown in figure 1(a), the damage peak moves deeper as the ion energy increases. The calculated damage profiles show a peak at around 0.15 μm, 0.65 μm and 1.1 μm and extend up to 0.5 μm, 1.2 μm and 1.8 μm for 1, 3 and 6 MeV, respectively. Detailed parameters of the heavy-ion irradiation are shown in Table 1. Moreover, a small amount of Cu impurity is introduced in the W sample as shown in figure 1(b), below 2×10^{-2} at.%. This Cu concentration is much lower than the impurity content in the pristine W material such as carbon (C), oxygen (O), and molybdenum (Mo) [28]. Moreover, a recent study reported that D retention in a Cu-damaged W sample with a damage level of 0.5 dpa does not differ from D retention in a self-damaged W sample [18]. Therefore, the effect of Cu impurities on D retention in our Cu-damaged W samples is considered to be negligible.

Table 1: Experiment parameters of Cu ion irradiation and D plasma exposure.

	Cu ion irradiation			D plasma exposure
Sample	Energy (MeV)	Dose (Cu/m^2)	dpa	Ion energy: 40 eV
1 MeV	1	3.75×10^{18}	0.5	Temperature: 550 ± 10 K
3 MeV	3	4.60×10^{18}	0.5	Flux: 1×10^{22} ions $m^{-2}s^{-1}$
6 MeV	6	5.30×10^{18}	0.5	Fluence: 1×10^{26} ions m^{-2}

After that, W samples with Cu irradiation were exposed to D plasma, which was performed in the linear plasma device STEP at Beihang University [29,30]. The electron density and electron energy of D plasma are relatively homogeneous within a diameter of 25 mm in STEP.

The exposed area is defined by a Mo holder with an opening of 8 mm × 16 mm. Hence, the D plasma homogeneously covers the exposed surface during exposure. In a single exposure experiment, two samples are exposed simultaneously, and the average exposed area of a single sample is ~64 mm^2. The incident ion energy was set as ~40 eV, by applying a negative bias voltage, and the ion flux was 1×10^{22} ions $m^{-2}s^{-1}$ as measured by a Langmuir probe located at 3.5 cm in front of the sample surface [9]. A total D fluence of 1×10^{26} ions m^{-2} was applied. The sample temperature measured by a K-type thermocouple was 550 ± 10 K. This temperature was chosen since blistering and retention in W were most severe at around 550 K with the plasma flux of 10^{22} $m^{-2}s^{-1}$ [20].

Surface morphology was observed using an optical microscope (OM, Carl Zeiss) and a scanning electron microscope (SEM, TESCAN LYRA3). A focused ion beam (FIB) was used to obtain the sub-surface morphology, where the cross-section was cut and polished by a Ga ion beam with an energy ranging from 10 to 30 keV.

Depth profiles of D were measured by NRA using the nuclear reaction $D(^3He, p)^4\alpha$ at the 3 MV tandem accelerator at the Max-Planck-Institut für Plasmaphysik (IPP) in Garching [15,31]. A ^3He ion beam with eight energies ranging from 0.5 to 4.5 MeV allows quantifying D within the first 7.4 μm from the surface. The NRA measurement spot was placed about 1 mm below the center of the plasma exposure area. This spot is selected after a lateral scan with an interval of about 2 mm by a 4.5 MeV beam, which was performed to check the lateral uniformity of the D concentration. Emitted protons were detected at a reaction angle of 135° and 175° for all energies in addition to alphas at a reaction angle of 102° for energies below 1.2 MeV. More details on the NRA setup are described in [15]. The decomposition of the measured proton and alpha spectra was performed using the NRADC software [32] to derive the most probable D concentration as a function of depth. Due to better counting statistics the proton spectra of the large angle counter placed at a reaction angle of 135° were analyzed. For the given measurement parameters, the sensitivity limit is then about 10^5 D/W. The reproducibility of the beam current measurement is typically 3–5%. Counting statistics for all three samples are below 1%, which can ensure that the repeatability of our measurements is within 5% [15]. Moreover, the absolute accuracy depends on the accuracy of the cross section which is also ~5% [33]. The absolute error bar for D retention measured by NRA is set at 10% in this work.

The TDS measurements were used to gain information on D trapping sites and total D retention. The W sample with D plasma exposure was placed in an ultra-high vacuum chamber (< 10^{-5} Pa), and heated up to 1273 K at a constant heating rate of 1 K/s and held for 3 min at 1273 K. Meanwhile, signals of mass 3 (HD) and mass 4 (D_2) were detected by a quadrupole mass spectrometer (QMS). The signal of mass 3 was calibrated by averaging the calibration of mass 2 and mass 4, and the signal of mass 4 was calibrated by a D_2 calibration leak from Vacuum Technology, Inc. (VTI) with a specified leak rate of 2.03×10^{-6} atm-cc/s and a stated accuracy of ~5 %. The measured signals were then converted to calibrated signals in the unit of particle number per square meter per second by using the before mentioned plasma exposed surface area. The uncertainty of the calibrated signal is ~5%, which is set as the error bar for total D retention measured by TDS. The total D retention consists of D_2 and HD, and the contribution of HD to the retention is usually less than 10 %. In this work, only the D_2 desorption spectrum is shown to demonstrate the desorption characteristics of each sample, while the HD spectrum is not presented due to its weak desorption strength.

3. Results

3.1 Surface and sub-surface morphology

Figure 2 shows the surface morphology of the damaged W samples exposed to D plasma with a fluence of 1×10^{26} m^{-2} and a temperature of 550 K. After D plasma exposure, dense blisters of various sizes and irregular shapes are observed on the surface of the W samples. It is worth noting that the density of blisters in the 1 MeV sample is higher than that in the 3 MeV and 6 MeV samples.

Although the OM and SEM images clearly indicate that the blister density decreases as the damage depth increases, further statistics are needed to quantify the influence of damage depth on the change in the blister density. Basically, a bulge is identified as a blister according to its shape and height-to-diameter ratio. Two main types are considered: flat-shaped blisters and dome-shaped blisters [34]. In the SEM image of 1 MeV sample (figure 2 (a)), flat-shaped and dome-shaped blisters are marked by red and orange circles, respectively. These features of blisters can be regarded as important bases for the counting process of the blister density. The size and number of blisters were counted in an area of ~0.84 mm^2 using five low-magnification

SEM images, in which the blister size is determined by the diameter of the equivalent circle. The result is shown in figure 3. In the cases of 1, 3, and 6 MeV, the number of blisters is 683, 188, and 161, respectively. About 60% of blisters are of a diameter of fewer than 10 μm, while the maximum diameter is ~75 μm. Meanwhile, using the statistics of diameters in figure 3 and assuming a blister to be an ideal circle, the total area of blisters in all samples is estimated. The total blister area is ~0.101 mm^2, ~0.054 mm^2, ~0.049 mm^2 for 1 MeV, 3 MeV and 6 MeV samples, respectively (within the area of ~0.84 mm^2). Such a result corresponds well to the intuitive observation of low-magnification OM images in figure 2 and the statistics of blister counts in figure 3. From the above results, it can be ensured that if the damage depth is changed the density of the blister will change accordingly.

Besides, as mentioned in the introduction, some relatively large-sized blisters will be formed in the damaged case compared with the undamaged one [12,20,21]. However, this phenomenon does not seem to become more prominent as the damage depth increases because no larger size blisters are observed in the 6 MeV case compared with the 1 and 3 MeV cases. Therefore, one can draw the conclusion that it is not that the deeper the damage depth, the larger the size of blisters will be formed in the damaged samples.

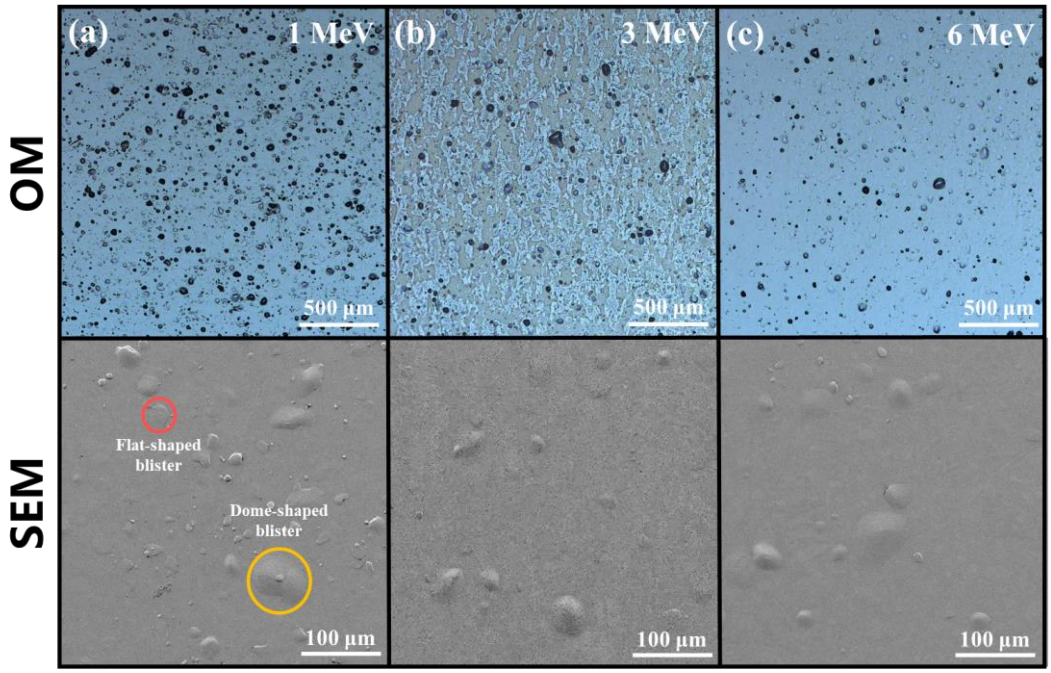

Figure 2. Surface morphology with low-magnification (OM, upper row) and high-magnification (SEM, lower row) of three W samples after exposure to D plasma. From left to

right: (a) 1 MeV, (b) 3 MeV, and (c) 6 MeV Cu energy. The slight erosion features on the surface observed in the 3 MeV sample may be due to the electropolishing process, but it does not disturb the observation of blisters. Two typical types of the blister with a flat shape and a dome shape are marked by red and orange circles, respectively, in the case of 1 MeV Cu irradiation.

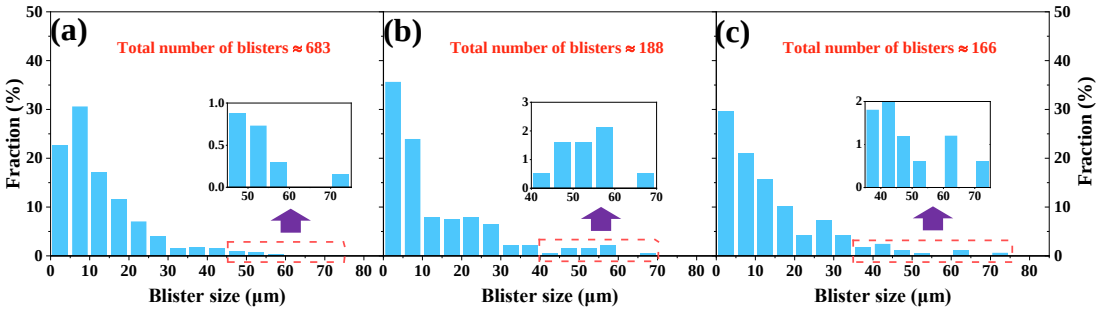

Figure 3. Distribution of blister size and number in 1 MeV (a), 3 MeV (b), and 6 MeV (c) sample. In each sample, blisters are counted in an area of ~0.84 mm^2.

3.2 Deuterium depth distribution

D depth profiles in the three W samples are displayed in figure 4(a) together with the statistical error bars derived from the deconvolution. Three distinct features are visible in this figure: First, the maximum D concentration close to the surface is similar in all three cases between 0.5 and 0.8 at.%. Second, the depth of this zone with maximum concentration increases with Cu ion energy. Third, the concentration at a larger depth is also similar for all three samples but about one order of magnitude smaller. In addition to an enlarged view of the D depth profiles the SRIM calculated primary radiation damage distribution is also shown for the three cases in figure 6(b)–(d). One can clearly see that the maximum depth of the enhanced D retention follows the calculated primary radiation damage as expected from literature. By integrating the D depth profiles, D retention within 7.4 μm in 1, 3, and 6 MeV samples is determined to be 5.2, 6.8, and 9.5×10^{20} D/m^2, respectively.

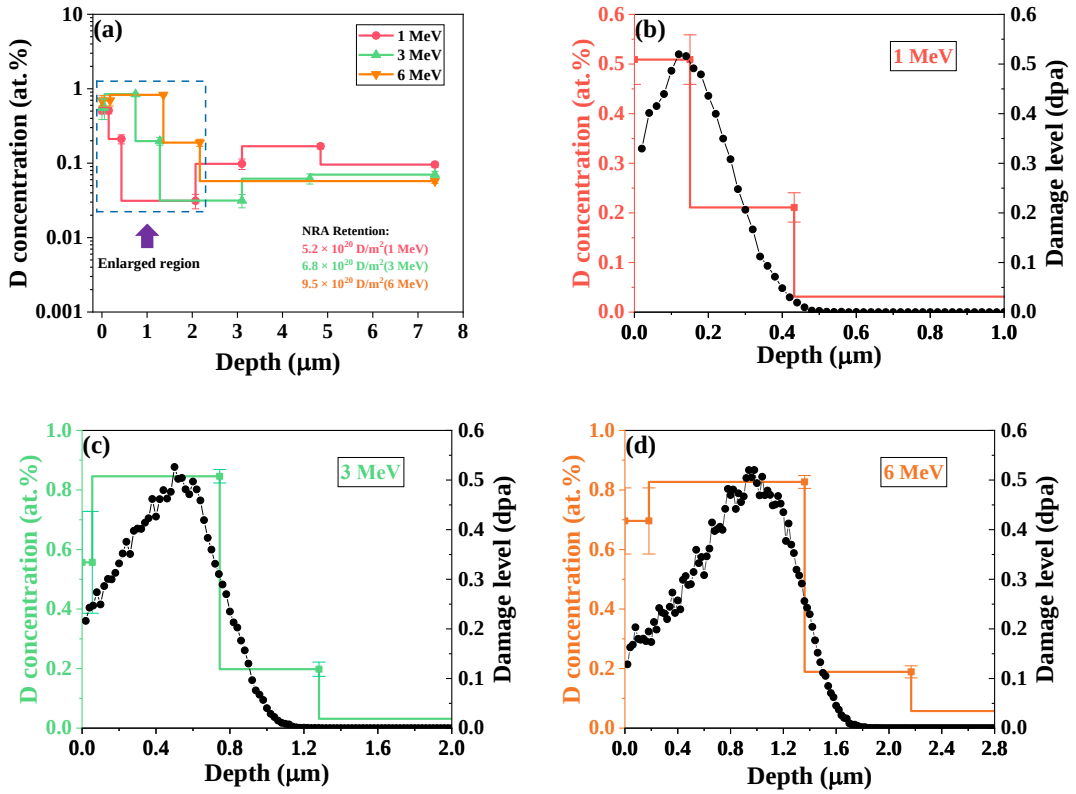

Figure 4. (a) D depth profiles in W samples after exposure to D plasma at 550 K. Enlarged D depth profiles are shown together with the calculated damage level for 1 MeV (b), 3 MeV (c), and 6 MeV (d) sample. The slight increase of D concentration after 3 μm is observed in the 1 MeV and 3 MeV cases. A similar phenomenon has been reported in previous studies [21,35]. We attitude this to two factors: (1) D_2 exists in the cavity of inter-granular blisters; (2) D atoms are trapped at defects introduced by the inter-granular blisters at different depths.

3.2 Deuterium desorption and retention

TDS profiles of the three investigated W samples are shown in figure 5. One main desorption peak at ~680 K and a small shoulder at a higher temperature of ~800–950 K are observed in all damaged samples. Although the desorption curves remain relatively similar in shape in all damaged cases, the initial desorption temperature is slightly higher in the case of 1 MeV than in the 3 and 6 MeV cases. This might be caused by a slight temperature fluctuation during the D plasma exposure. As expected, the intensity of the desorption peak increases as the damage depth increases. Total D retention is 5.8, 8.3, and 16.2×10^{20} D/m^2 for 1, 3, and 6 MeV samples, respectively. This is in line with literature where the increase of total D retention in W is attributed to the large number of trap sites introduced by the MeV ion irradiation [12,14,36].

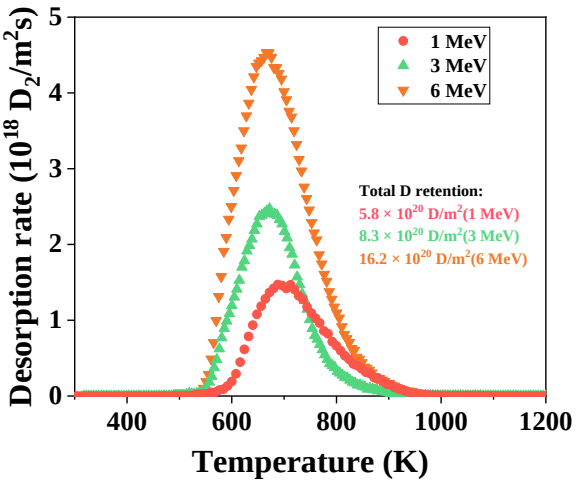

Figure 5 TDS profiles of the three W samples after exposure to D plasma at 550 K.

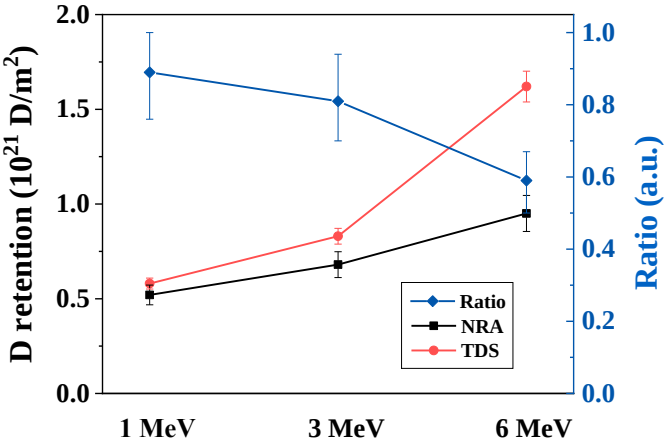

Figure 6 D retention measured by NRA and TDS. The ratio of D retention by NRA to D retention by TDS is also shown. Solid lines only guide the eye.

To gain information about D retention at depth larger than 7.4 μm, the partial (< 7.4 μm as measured by NRA) and total D retention (as measured by TDS) in the three investigated W samples are compared in figure 6. It can be seen that the difference between NRA and TDS results becomes larger as the Cu ion energy increases. This suggests that D retention at depths larger than 7.4 μm, which is not detected by the NRA, increases as the damage depth increases. Enhanced D retention in damaged samples at depths larger than SRIM prediction was not investigated in detail in literature so far. It might be attributed to the diffusion or generation of damage-induced defects beyond the capability of SRIM calculation [37] at first sight. However,

a good agreement of the measured damage-induced defect depth with SRIM calculation in W has been reported by Ł. Ciupiński et al. [38]. Furthermore, the maximum depth of retention is roughly estimated by dividing the D retention beyond 7.4 μm (retention using TDS subtracted by retention using NRA) by the D concentration at a depth of ~7.4 μm, which is ~7.4–9.7 μm, ~10.6–15.6 μm, ~29.1–38.8 μm in the 1 MeV, 3 MeV, and 6 MeV samples, respectively. The range of maximum depth is given according to the error bar in TDS and NRA measurement. These results indicate that there must be factors other than damage-induced defects affecting D trapping and diffusion, which will be discussed in section 4.

4. Discussion

4.1 Reduction of the blister density with the increasing damage depth

In this work, it is found that the blister density declines in the damaged W samples with the extension of the damage depth. As blister formation is usually related to the solute D concentration which induces the critical stress required for blister or crack nucleation during plasma exposure (i.e. ~0.0035 at.% at 550 K) [39], the effect of ion damage on solute D concentration and D diffusion is first discussed.

The distribution of solute D in a plasma-exposed sample is usually divided into three primary regions from the surface to the rear [40]. The first region is within the ion-implantation depth (R_{imp}), where D ions with certain energy are implanted into W; the second region is within the blistering-relevant depth ($R_{blister}$), where D atoms diffuse from R_{imp} and thereby are trapped; the third region is the bulk (R_{bulk}) where there is little or even no D atoms due to the limited exposure conditions such as the exposure time and temperature. Normally, solute D diffuses from R_{imp} to $R_{blister}$ rapidly at the beginning of plasma exposure if there is no ion damage. Afterwards, solute D atoms at $R_{blister}$ aggregate at defects which gives rise to D oversaturation and then blister nucleation. In the case of damaged samples, both D diffusion from R_{imp} to the bulk and D aggregation during diffusion are slowed down [19], which results in dispersion and therefore reduction of solute D concentration in the ion damaged region determined by the Cu ion energy. Such an effect permits a postponed blister formation because only when the ion-damage induced defects are filled with D, the solute D concentration will be as high as in the undamaged case which could induce blister nucleation. However, this effect should vanish for

plasma exposures much longer than the time the D needs to diffuse through the damaged zone. As shown in our previous work [10] reduction of the blister density is still observed in the damaged W sample even at a high fluence of 2.27×10^{27} m^{-2} and a long exposure time of 30 hours. This effect can hence not explain the observation, but at least one thing can be deduced based on the above discussion: the time for the formation of the first blister is largely postponed in the damaged W sample compared with the undamaged one and will continue to be delayed as the damage depth extends.

Aside from the critical concentration of solute D, defects also play an important role in blister formation as the prerequisite for nucleation. In fact, the reduced blister density in the damaged W sample could be well explained based on a dislocation nucleation blister mechanism as recently proposed by Guo *et al.* [9]. The formation of <001> edge dislocation and dislocation tangles is suggested to trigger the crack nucleation as the initial stage of blister formation [9]. As a large number of vacancies and interstitial dislocation loops are formed during ion damage, the dislocation motion [41,42] and therefore the formation of dislocation tangles are strongly obstructed. This will reduce the number of blister nuclei and finally gives rise to the reduction of the blister density. Following this concept, it is not hard to understand that the reduction of blister density becomes more pronounced with a larger damage depth because the influence of displacement-damage defects on blister nuclei is deepened. Moreover, previous studies found that H can enhance the local plasticity of the material [43,44], which means that as the damage depth increases, a gradually elevated stress is required for crack nucleation in the damaged cases due to the continuously raised in D content in bulk.

4.2 Enhanced D retention at a depth larger than 7.4 μm with the increasing damage depth

The comparison of D retention between NRA and TDS measurements as shown in figure 6 allows drawing conclusions about D retention at depth larger than 7.4 μm. After exposure to D plasma with the here used conditions (flux = 1×10^{22} ions $m^{-2}s^{-1}$, fluence = 1×10^{26} ions m^{-2}, temperature = 550 K), the D retention at depth larger than 7.4 μm in the damaged W samples (measured by TDS) enhances as the damage depth increases. This is unlikely to be due to heavy-ion irradiation-induced defects. As the actual damage depth is found to agree with calculated damage depth [37,45], 7.4 μm is far beyond the damage depth even in the case of 6 MeV. Thus,

the enhanced D retention must be attributed to D trapping at intrinsic or plasma-induced defects at a depth beyond 7.4 μm. Considering the identical exposure time in all damaged cases, it can be speculated that the D diffusion flux beyond a depth of 7.4 μm in the damaged case is increased with the damage depth.

Along with the observation of the different blistering behavior - especially because of the reduced blister density in W samples with larger damage depth - different blistering is proposed to be responsible for the change of the D diffusion flux. As one of the most prominent modifications of the W surface morphology, blisters due to D plasma exposure with a low incident energy were observed more than twenty years ago [46,47] and widely investigated [1]. Recent studies provide details about how blistering increases the trapping of HIs and reduces the HIs diffusion flux in W [21,22]: (i) dislocations introduced by blistering can act as trap sites for HIs which increases HIs trapping and hinders the diffusion into the bulk [9,35,48,49]; (ii) an unruptured blister is very close to a quasi-infinite sink for HIs before it ruptures, which can be applied to infer indirectly that the unruptured blisters hinder the inward D diffusion during the plasma exposure [22]; (iii) once the blister ruptures, the ruptured blister cavity will connect to the surface which acts as an exit for HI and thereby reduces the net diffusion of HIs into the bulk [21]; (iv) the presence of blisters on the sample surface can lead to an increase in the probability of HIs re-emission from the surface, which is due to the rough surface caused by blistering. These detailed processes are shown via the 'MAGNIFIED DETAILS' in figure 7, which is modified based on the mechanism proposed by Schmid *et al.* [40]. From the above discussion, it can be concluded that whether a blister is ruptured or not, its influence on the transport of HIs into the bulk is suppression. And such suppression of HIs transportation by blister is embodied in a reduction of HIs diffusion flux into the bulk.

Considering the effect of blistering on HIs transport described above, a dependence of the D diffusion flux on the blister density is proposed in the damaged cases. According to the analysis of the Cu ion irradiation effect on the blistering process in section 4.1, the blistering incubation time in the damaged cases is very likely to be enlarged with extending the damage depth. Following this idea, the effect of blisters on D diffusion flux in the 1 MeV sample occurs earlier than in the 3 MeV and 6 MeV samples. That is, the D diffusion flux will be first reduced in W sample with a smaller damage depth as blistering happens at an earlier time. These

descriptions correspond to the first two stages of '$0 - t_1$' and '$t_1 - t_2$' in figure 7. As a result, the amount of D atoms reaching a depth beyond the blistering-relevant depth is lower in the 1 MeV case compared with the 6 MeV case under the same exposure time. Namely, the presence of blisters decreases the number of D that passes the blister-relevant region and diffuses into the bulk. In the third stage of '$t_2 - t_3$', the disparity of D flux between the 1, 3 and 6 MeV cases grows as the difference in the blister density increases. Once the blister density stabilizes, the D flux into the W bulk also tends to be constant corresponding to the last stage of '$t_3 - t_n$'. At this time, the D diffusion flux is largely determined by the blister density, which is well in line with the results obtained from OM and SEM observations, as well as NRA and TDS measurements. The fewer blisters form, the more D atoms will diffuse into larger depth (> 7.4 μm) and thus are captured by the existing traps, which finally results in the enhancement of retained D amount at an identical loading condition. Hence, it can be concluded that a gradually reduced blister density in the damaged cases permits a higher and higher D diffusion flux beyond the blistering-relevant depth.

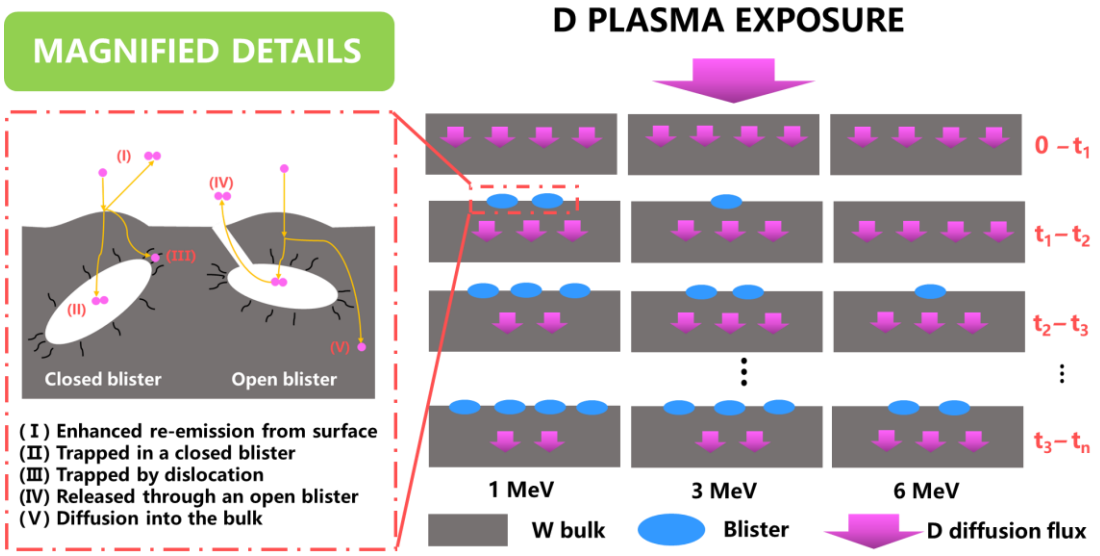

Figure 7. Schematic diagram of the effect of the blister density on the D diffusion flux in W. In the 'MAGNIFIED DETAILS', five processes related to the effect of a single blister on D transport are shown and described. Following the 'MAGNIFIED DETAILS', it is suggested that blisters play an obstructive role on the inward diffusion of D. Based on this, it is assumed that the zone corresponding to the blistering is regarded as the main region where the D inward diffusion flux is affected. '$0 - t_n$' represents the period from no blisters to blisters with a stable

density, including four main stages: ‘Blistering incubation’, ‘Start to blister’, ‘Blister density gradually increased’ and ‘Blister density gradually stabilized’. During these periods, the effect of the blister density on the D diffusion flux gradually functions and eventually reaches a constant.

The results in this work help to understand HIs transportation in W components in a future fusion device at temperatures relevant for blister formation. As the dpa rate of neutrons is low, plasma-induced blistering must happen before neutron-induced defect could interfere with blistering. Then an open question is that, whether the surface is covered by intact blisters all the time, or suffered from cycles of blister-formation and blister-removal due to combined ELMy and plasma irradiation during Tokamak operation. In the former case, a high density of blisters would cover the surface, a low HIs diffusion flux is expected [21] and the HIs filling rate at bulk defects is low. If it is the second case, once the blister nucleation is affected by neutron irradiation, an elevated HIs diffusion flux (but still lower than in the pristine W) is suggested due to the reduced blister density according to this work. This leads to an elevated HIs filling rate at the bulk defect, which could potentially accelerate global tritium retention. And this indicates not only the HIs trapping ability is increased, but also the HIs filling rate at bulk defects (HIs diffusion flux) may be changed due to neutron irradiation in future fusion devices.

5. Conclusion

The effect of the damage depth on blistering and D retention in W has been studied in this work. Cu ion irradiation with incident energies of 1, 3, and 6 MeV was utilized to produce samples with various damage depths at an identical peak damage level of 0.5 dpa. Then the W samples with the ion irradiation were exposed to D plasma with a low incident energy of 40 eV and a high flux of 1×10^{22} ions $m^{-2}s^{-1}$ at a temperature of 550 K. After exposure to D plasma, the density of blisters in the damaged W is reduced with increasing damage depth. Such a reduction of blister density is suggested to be attributed to the interference of displacement-damage defects on the dislocation tangle during blister nucleation in the damaged cases, namely the deeper the damage depth, the deeper the area at which blister nucleation is influenced by defects.

Besides, the formation of relatively large-sized blisters in the damaged sample compared with the undamaged one in previous studies [10,20] is independent of the damage depth.

As expected, the D retention within the damage layer is increased with the increasing damage depth in the damaged W samples. However, as the damage depth extends, an unexpected enhanced D retention at a depth larger than 7.4 μm (far beyond the calculated damage depth by SRIM) in damaged samples is revealed by the difference of D retention measured by TDS and NRA. The reduced blister density that is the consequence of the damage depth is proposed as the dominant effect for the enhanced D diffusion flux.

Acknowledgments

This work was supported by the National MCF Energy R&D Program under Grant No. 2019YFE03110100 and the National Natural Science Foundation of China under Grant No. 51720105006, 11805007, 11775015, 11905140 and 12075020. Prof. Engang Fu is grateful to be fund by National Magnetic Confinement Fusion Energy Research Project under Grant No. 2017YFE0302500 and 2018YFE0307100. Shiwei Wang would like to thank Dr. Liang Gao from Forschungszentrum Jülich GmbH and Dr. Wolfgang Jacob from IPP-Garching for the valuable discussions of the mechanism covered in this article and Dr. Chuan Xu for the technical assistance in the heavy-ion irradiation in Ion Beam Materials Lab at Peking University.

Reference

[1] De Temmerman G, Hirai T and Pitts R A 2018 The influence of plasma-surface interaction on the performance of tungsten at the ITER divertor vertical targets *Plasma Phys. Control. Fusion* **60**

[2] Lu G H, Zhou H B and Becquart C S 2014 A review of modelling and simulation of hydrogen behaviour in tungsten at different scales *Nucl. Fusion* **54**

[3] Ueda Y, Schmid K, Balden M, Coenen J W, Loewenhoff T, Ito A, Hasegawa A, Hardie C, Porton M and Gilbert M 2017 Baseline high heat flux and plasma facing materials for fusion *Nucl. Fusion* **57**

[4] Rieth M, Doerner R, Hasegawa A, Ueda Y and Wirtz M 2019 Behavior of tungsten under irradiation and plasma interaction *J. Nucl. Mater.* **519** 334–68

[5] Hatano Y, Shimada M, Otsuka T, Oya Y, Alimov V K, Hara M, Shi J, Kobayashi M, Oda T, Cao G, Okuno K, Tanaka T, Sugiyama K, Roth J, Tyburska-Püschel B, Dorner J, Yoshida N, Futagami N, Watanabe H, Hatakeyama M, Kurishita H, Sokolov M and Katoh Y 2013 Deuterium trapping at defects created with neutron and ion irradiations in tungsten *Nucl. Fusion* **53** 073006

[6] Alimov V K, Hatano Y, Kuwabara T, Toyama T, Someya Y and Spitsyn A V. 2020 Deuterium release from deuterium plasma-exposed neutron-irradiated and non-neutron-irradiated tungsten samples during annealing *Nucl. Fusion* **60**

[7] Condon J B and Schober T 1993 Hydrogen bubbles in metals *J. Nucl. Mater.* **207** 1–24

[8] Liu Y-L, Zhang Y, Zhou H, Lu G, Liu F and Luo G-N 2009 Vacancy trapping mechanism for hydrogen bubble formation in metal *Phys. Rev. B* **79** 172103

[9] Guo W, Ge L, Yuan Y, Cheng L, Wang S, Zhang X and Lu G-H 2019 <001> edge dislocation nucleation mechanism of surface blistering in tungsten exposed to deuterium plasma *Nucl. Fusion* **59** 026005

[10] Wang S, Zhu X, Cheng L, Guo W, Liu M, Xu C, Yuan Y, Fu E, Cao X Z and Lu G H 2018 Effect of heavy ion pre-irradiation on blistering and deuterium retention in tungsten exposed to high-fluence deuterium plasma *J. Nucl. Mater.* **508** 395–402

[11] Zhu X-L, Zhang Y, Cheng L, Shi L-Q, De Temmerman G, Yuan Y, Liu H-P and Lu G-H 2018 Suppression of deuterium-induced blistering in pre-damaged tungsten exposed to short-duration deuterium plasma *J. Nucl. Mater.* **500** 295–300

[12] 'T Hoen M H J, Balden M, Manhard A, Mayer M, Elgeti S, Kleyn A W and Zeijlmans Van Emmichoven P A 2014 Surface morphology and deuterium retention of tungsten after low- and high-flux deuterium plasma exposure *Nucl. Fusion* **54**

[13] Zhu X L, Cheng L, Wang S W, Yuan Y, Lu G H, Zhang Y, Lu E Y, Cao X Z and Huang J J 2019 Reduced blister quantity in damaged tungsten exposed to deuterium plasma *Sci. China Physics, Mech. Astron.* **62** 957021

[14] Zhu X-L, Zhang Y, Cheng L, Yuan Y, De Temmerman G, Wang B-Y, Cao X-Z and Lu G-H 2016 Deuterium occupation of vacancy-type defects in argon-damaged tungsten exposed to high flux and low energy deuterium plasma *Nucl. Fusion* **56** 036010

[15] Schwarz-Selinger T, Bauer J, Elgeti S and Markelj S 2018 Influence of the presence of deuterium on displacement damage in tungsten *Nucl. Mater. Energy* **17** 228–34

[16] T'Hoen M H J, Tyburska-Püschel B, Ertl K, Mayer M, Rapp J, Kleyn A W W, Van Emmichoven P A Z, Hoen M H J 't, Tyburska-Püschel B, Ertl K, Mayer M, Rapp J, Kleyn A W W, Zeijlmans van Emmichoven P A, T'Hoen M H J, Tyburska-Püschel B, Ertl K, Mayer M, Rapp J, Kleyn A W W and Van Emmichoven P A Z 2012 Saturation of deuterium retention in self-damaged tungsten exposed to high-flux plasmas *Nucl. Fusion* **52** 023008

[17] Markelj S, Schwarz-Selinger T, Pečovnik M, Založnik A, Kelemen M, Čadež I, Bauer J, Pelicon P, Chromiński W and Ciupinski L 2019 Displacement damage stabilization by hydrogen presence under simultaneous W ion damage and D ion exposure *Nucl. Fusion* **59**

[18] Wielunska B, Mayer M, Schwarz-Selinger T, Sand A E and Jacob W 2020 Deuterium retention in tungsten irradiated by different ions *Nucl. Fusion* **60** 096002

[19] Barton J L, Wang Y Q, Doerner R P and Tynan G R 2016 Model development of plasma implanted hydrogenic diffusion and trapping in ion beam damaged tungsten *Nucl. Fusion* **56** 106030

[20] Zhu X L, Zhang Y, Kreter A, Shi L Q, Yuan Y, Cheng L, Linsmeier C and Lu G H

2018 Aggravated blistering and increased deuterium retention in iron-damaged tungsten after exposure to deuterium plasma with various surface temperatures *Nucl. Fusion* **58**

[21] Bauer J, Schwarz-Selinger T, Schmid K, Balden M, Manhard A and Von Toussaint U 2017 Influence of near-surface blisters on deuterium transport in tungsten *Nucl. Fusion* **57**

[22] Gao L, Von Toussaint U, Jacob W, Balden M and Manhard A 2014 Suppression of hydrogen-induced blistering of tungsten by pre-irradiation at low temperature *Nucl. Fusion* **54**

[23] Wang S, Guo W, Yuan Y, Gao N, Zhu X, Cheng L, Cao X, Fu E, Shi L, Gao F and Lu G H 2020 Evolution of vacancy defects in heavy ion irradiated tungsten exposed to helium plasma *J. Nucl. Mater.* **532** 152051

[24] Stoller R E, Toloczko M B, Was G S, Certain A G, Dwaraknath S and Garner F A 2013 On the use of SRIM for computing radiation damage exposure *Nucl. Instruments Methods Phys. Res. Sect. B Beam Interact. with Mater. Atoms* **310** 75–80

[25] Ziegler J F, Ziegler M D and Biersack J P 2010 SRIM - The stopping and range of ions in matter (2010) *Nucl. Instruments Methods Phys. Res. Sect. B Beam Interact. with Mater. Atoms* **268** 1818–23

[26] Ziegler J F, Ziegler M D and Biersack J P SRIM - The Stopping and Range of Ions in Matter, SRIM co., Chester, Maryland, USA, 2008. www.srim.org.

[27] ASTM Int'l E521-96(2009) Standard Practice for Neutron Radiation Damage Simulation by Charge-Particle Irradiation, Annual Book of ASTM Standards Vol 12.02 (Philadelphia, PA: American Society for Testing and Materials) p 7.

[28] ATTL Advanced Materials Co., Ltd. China www.tlwm.cn

[29] Lu G H, Cheng L, Arshad K, Yuan Y, Wang J, Qin S, Zhang Y, Zhu K, Luo G N, Zhou H, Li B, Wu J and Wang B 2017 Development and optimization of STEP-A linear plasma device for plasma-material interaction studies *Fusion Sci. Technol.* **71** 177–86

[30] Yin H, Wang J, Guo W, Cheng L, Yuan Y and Lu G 2019 Recent studies of tungsten-based plasma-facing materials in the linear plasma device STEP *Tungsten* **1** 132–40

[31] Wielunska B, Mayer M, Schwarz-Selinger T, Von Toussaint U and Bauer J 2016 Cross section data for the D(3He,p)4He nuclear reaction from 0.25 to 6 MeV *Nucl. Instruments Methods Phys. Res. Sect. B Beam Interact. with Mater. Atoms* **371** 41–5

[32] Schmid K and Von Toussaint U 2012 Statistically sound evaluation of trace element depth profiles by ion beam analysis *Nucl. Instruments Methods Phys. Res. Sect. B Beam Interact. with Mater. Atoms* **281** 64–71

[33] Möller W and Besenbacher F 1980 A note on the 3He + D nuclear-reaction cross section *Nucl. Instruments Methods* **168** 111–4

[34] Xu H Y, Liu W, Luo G N, Yuan Y, Jia Y Z, Fu B Q and De Temmerman G 2016 Blistering on tungsten surface exposed to high flux deuterium plasma *J. Nucl. Mater.* **471** 51–8

[35] Liu M, Guo W, Cheng L, Wang J, Wang S, Yin H, Wang T, Huang Y-H, Yuan Y, Schwarz-Selinger T, Temmerman G De, Cao X Z, Luo G N and Lu G H 2020 Blister-

dominated retention mechanism in tungsten exposed to high-fluence deuterium plasma *Nucl. Fusion* **60**

[36] Zinkle S J and Snead L L 2018 Opportunities and limitations for ion beams in radiation effects studies: Bridging critical gaps between charged particle and neutron irradiations *Scr. Mater.* **143** 154–60

[37] Zhang Z, Yabuuchi K and Kimura A 2016 Defect distribution in ion-irradiated pure tungsten at different temperatures *J. Nucl. Mater.* **480** 207–15

[38] Ciupiński Ł, Ogorodnikova O V, Płociński T, Andrzejczuk M, Rasiński M, Mayer M and Kurzydłowski K J 2013 TEM observations of radiation damage in tungsten irradiated by 20MeV W ions *Nucl. Instruments Methods Phys. Res. Sect. B Beam Interact. with Mater. Atoms* **317** 159–64

[39] Gao L, Manhard A, Jacob W, Von Toussaint U, Balden M and Schmid K 2019 High-flux hydrogen irradiation-induced cracking of tungsten reproduced by low-flux plasma exposure *Nucl. Fusion* **59**

[40] Schmid K, Bauer J, Schwarz-Selinger T, Markelj S, Toussaint U V., Manhard A and Jacob W 2017 Recent progress in the understanding of H transport and trapping in W *Phys. Scr.* **2017**

[41] Was G S 2017 The Radiation Damage Event *Fundamentals of Radiation Materials Science* (New York, NY: Springer New York) pp 3–76

[42] Hu X, Koyanagi T, Fukuda M, Kumar N A P K, Snead L L, Wirth B D and Katoh Y 2016 Irradiation hardening of pure tungsten exposed to neutron irradiation *J. Nucl. Mater.* **480** 235–43

[43] Birnbaum H K and Sofronis P 1994 Hydrogen-enhanced localized plasticity—a mechanism for hydrogen-related fracture *Mater. Sci. Eng. A* **176** 191–202

[44] Liang Y, Sofronis P and Dodds R H 2004 Interaction of hydrogen with crack-tip plasticity: Effects of constraint on void growth *Mater. Sci. Eng. A* **366** 397–411

[45] Yi X, Jenkins M L, Hattar K, Edmondson P D and Roberts S G 2015 Characterisation of radiation damage in W and W-based alloys from 2 MeV self-ion near-bulk implantations *Acta Mater.* **92** 163–77

[46] Ye M Y, Kanehara H, Fukuta S, Ohno N and Takamura S 2003 Blister formation on tungsten surface under low energy and high flux hydrogen plasma irradiation in NAGDIS-I *J. Nucl. Mater.* **313**–**316** 72–6

[47] Sze F C, Doerner R P and Luckhardt S 1999 Investigation of plasma exposed W-1% La2O3 tungsten in a high ion flux, low ion energy, low carbon impurity plasma environment for the International Thermonuclear Experimental Reactor *J. Nucl. Mater.* **264** 89–98

[48] Chen W Q, Wang X Y, Chiu Y L, Morgan T W, Guo W G, Li K L, Yuan Y, Xu B and Liu W 2020 Growth mechanism of subsurface hydrogen cavities in tungsten exposed to low-energy high-flux hydrogen plasma *Acta Mater.* **193** 19–27

[49] Manhard A, von Toussaint U, Balden M, Elgeti S, Schwarz-Selinger T, Gao L, Kapser S, Płociński T, Grzonka J, Gloc M and Ciupiński 2017 Microstructure and defect analysis in the vicinity of blisters in polycrystalline tungsten *Nucl. Mater. Energy* **12** 714–9